PCCP

Accepted Manuscript

ROYAL SOCIETY OF CHEMISTRY

www.rsc.org/pccp

Cite this: DOI: 10.1039/c0xx00000x

www.rsc.org/xxxxxx

ARTICLE TYPE

Electronic structure and conformational flexibility of D-cycloserine

Antonello Filippi,[a] Caterina Fraschetti,[a] Felice Grandinetti,[b] Maurizio Speranza,[a] Aurora Ponzi,[c] Piero Decleva,[c] Stefano Stranges,[a,d] **

Received (in XXX, XXX) Xth XXXXXXXXX 20XX, Accepted Xth XXXXXXXXX 20XX

DOI: 10.1039/b000000x

Abstract

*The first comprehensive investigation of the role played by the conformational flexibility of gaseous D-cycloserine in the valence and core electronic structures is here reported. The seven most stable conformers among the twelve structures calculated at MP2/6-311++G** level of theory were assumed to properly describe the properties of the investigated compound. Taking into account the contribution of these isomers, the valence photoelectron spectrum (UPS) was simulated by the Outer Valence Green's Function (OVGF) method. A different sensitivity to the conformational flexibility of the outermost photoelectron bands was exhibited in the simulated spectrum. The comparison of the theoretical UPS with the experimental one allowed a detailed assignment of the outermost valence spectral region. The composition and bonding properties of the relevant MOs of the most stable conformers were analyzed in terms of leading Natural Bond Orbitals (NBOs) contributions to the HF/6-311++G** canonical MOs. The C1s, N1s, and O1s photoelectron spectra (XPS) were theoretically simulated by calculating the vertical Ionization Energies (IEs) of the relevant conformers using the ΔSCF approach. The different IE chemical shift spread of the XPS components associated to the various conformers, which is expected to affect the experimental spectra, could be evaluated in the simulated XPS, thus providing new insight into the core electronic structure. The comparison of the theoretical results with the experiment unraveled that the atomic XPS components are not mixed by the D-cycloserine conformational flexibility, and that the specific vibronic structure of the different spectral components should play a crucial role in determining the different relative intensities and band shapes observed in the experiment.*

Keywords:

cycloserine, conformers, MO analysis, electronic structure, UPS, XPS, MP2, OVGF, ADF, SCF

1. Introduction

D-Cycloserine ((*R*)-4-amino-1,2-oxazolidin-3-one) is a drug FDA-approved under the name of Seromycin®. It is used as a broad-spectrum antibiotic in a second line treatment of tuberculosis,[1] and due to its action on N-methyl-D-aspartate (NMDA) receptors, it is also employed in the clinical treatments of anxiety,[2-5] and obsessive-compulsive disorders.[6,7] Since its commercial availability in 1952, numerous studies addressed the biological efficacy of cycloserine, but its physicochemical properties are only little explored.[8,9] Despite the activity toward the NMDA receptors is thought to be determined by its HOMO (Highest Occupied Molecular Orbital) and LUMO (Lowest Unoccupied Molecular Orbital),[10] the electronic structure of D-cycloserine, and its dependence on conformational effects, are still essentially uncovered. Some insights in this regard were recently obtained by Ultraviolet and X-ray Photoelectron Spectroscopies (UPS and XPS), and DFT calculations.[11] Two conformers of D-cycloserine were assumed to predominate in the gas phase, namely III and VII, separated in energy by 1.1 kcal mol^{-1}(Fig. 1). However, the valence and core ionization spectra, simulated by assuming this binary mixture, did not result in good agreement with the experiment. This is explained, in the light of the results reported in the present work, by the fact that the two minor conformers III and VII cannot be considered the predominant species in the gas phase, and that the molecular flexibility is not only affected by the rotation of the NH_2 group around the N-C adjacent bond, but other structural degrees of freedom have to be considered to properly describe the molecular properties of D-cycloserine.

Quite recently, in fact, some of us performed a detailed investigation on the structure of D-cycloserine and its protomers in the unsolvated state.[12] Besides III and VII, ten other conformers were identified on the MP2/6-311++G** potential energy surface (PES) of D-cycloserine, some of them being significantly more stable than III and VII (e.g. I and II in Fig.1). Based on these findings, we felt appropriate to re-examine the valence and core photoelectron spectra of D-cycloserine taking properly into account its full set of conformational degrees of freedom.

2. Computational methods and details

2.1 Optimized conformational geometries and relative stabilities

The geometries of the various conformers of the D-cycloserine were fully optimized at the MP2(fc)[13] level of

theory, using the 6-311++G** split-valence basis set. The twelve located structures, shown in Fig. 1 (see also supplementary material b)), can be grouped into four sets of three conformers (rotamers), each member of any set being obtained by rotating the NH_2 moiety around the C_4-N_7 bond axis. Thus, the four groups of

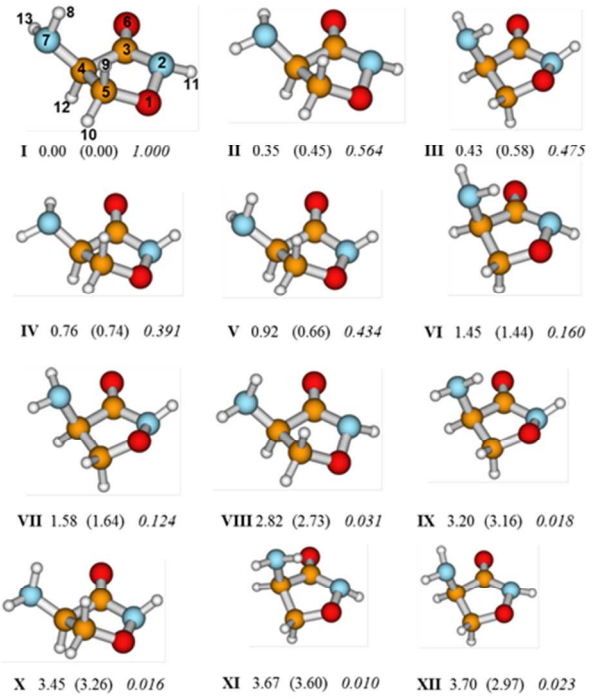

Fig.1 Schematic pictures of the MP2/6-311++G** optimized structures of the twelve conformers (I-XII) of D-cycloserine. Atom labelling is given in structure I. The relative enthalpy (normal) and free energy (parenthesis) are in kcal mol^{-1}, and the Boltzmann population (italics) are calculated at 395 K.

rotamers correspond to the four different ring conformations generated by combining the two puckering of the isoxazolidine ring O_1-*exo*-C_5-*endo* and O_1-*endo*-C_5-*exo* (see supplementary material a)), with the axial and equatorial orientations of the N_2-H bond in the isoxazolidine ring. The inspection of Fig. 1 allows to identify the groups of the rotamers as (I-II-VIII), (III-VII-IX), (IV-V-X), and (VI-XI-XII). In particular, the two most stable conformers I and II correspond to the ring puckering O_1-*exo*-C_5-*endo* with the equatorially-oriented N_2-H bond, and are structurally related by an approximately 120° rotation of the NH_2 moiety around the C_4-N_7 bond.

The located conformers were ascertained to be local minima on the MP2(fc)/6-311++G** PES by calculating their harmonic vibrational frequencies at this level. The obtained values were also employed to estimate the zero-point energies, and the thermal corrections to enthalpy and free energy at 395 K. To this end, we employed standard statistical thermodynamics, within the approximations of harmonic oscillator, rigid rotor, and ideal gas to describe, respectively, the vibrations, rotations, and translations of the real systems. Relative Gibbs free energies were used to assess the Boltzmann populations at T = 395K (only conformers with a relative population greater than 0.100 were taken into account).

The calculations were performed with the 1 MAY 2012 (R1) release of GAMESS,[14,15] installed on a six-core (8 Intel-Xeon E5520 2.27 GHz CPU and 24 GB DDR3 RAM each) cluster (48 CPU total), and ran under a Debian GNU/Linux 6.04 operating system. The present MP2 calculations used an improved basis set with respect to our previous work (MP2(fc)/6-311+G**).[12] Furthermore, for comparative purpose, the twelve optimized conformational geometries and their relative energies were also obtained by the same method of Ref.11. These latter results are not shown here since the spectral simulations based on optimized geometries and energies obtained by the MP2 calculations resulted in a slightly better agreement with the experiment than that of the theoretical simulations derived by the B3LYP/6-311++G** method.

2.2 Valence Ionization Energy calculations and MO analysis

The IEs of the outer-valence (< 20 eV) MOs and their (relative) intensities (pole strengths) were calculated using the OVGF method[16-20] as implemented in Gaussian 03.[21] The calculations were performed at the MP2/6-311++G** optimized geometries.

The composition of the valence MOs was assayed by analyzing the HF/6-311++G** canonical (delocalized) MOs in terms of their leading Natural Bond Orbitals (NBOs) contributions.[22] These calculations were performed using the canonical MO analysis routine implemented in the GENNBO 6.0W program.[23] Within this approach, each canonical MO (φ_i) is expressed in terms of the complete orthonormal set of NBO's $\{\Omega_\alpha\}$ by the equation $\varphi_i = \sum_\alpha \Omega_\alpha c_{\alpha i}$. The coefficients $c_{\alpha i}$ (elements of the MO-NBO transformation matrix) determine the percentage contribution ($100\times|c_{\alpha i}|^2$) of each NBO to the MO-NBO expansion of φ_i. Each coefficient $c_{\alpha i}$ can in turn be identified with a NBO Ω_α of bonding, nonbonding, or antibonding character. By adding the percentage contributions of each NBO type, one obtains a measure of the total bonding, non-bonding, or antibonding character of each MO.

2.3 Core Ionization Energies

The density functional theory (DFT) calculations of core IEs were performed for all the relevant conformers of D-cycloserine using the ADF code,[24-26] and the TZP basis set from the ADF database. Two approaches have been used. In the first case, the LB94 potential was employed, and the IEs were simply obtained as negative energy eigenvalues, in the same spirit of Koopmans Theorem (KT). It is well known that KT is not strictly valid in DFT, but experience has shown that LB94 eigenvalues give a fair approximation to core IEs, without employing separate calculations for the ion.[27] In the second case, since the aim of the present study focuses on the accurate description of the relative order and chemical shifts of the IEs, the ΔSCF approach has been employed to obtain the IE values. Separate SCF calculations on the neutral ground state and the ionized molecule have been performed employing the PW86/PW91c exchange and correlation potential included in ADF, and a spin polarized calculation. This was also the recommended choice in a former extensive investigation of DFT approaches for core IEs.[28] Hole localization is easily achieved thanks to the possibility in ADF to employ atomic fragments to build the molecule, with a core hole atom fragment on the desired site.

Table 1 Analysis of the HF/6-311++G** canonical MOs of D-cycloserine (conformers I-VII) in terms of their leading NBO contributions

MO	Conf.	Leading NBO Contributions[1]	Character[2]
HOMO (20*a*)	I	0.483 *n*(N7) + 0.436 *n*(N2) - 0.422 *n*(O6) - 0.373 *n*(O1) + 0.311 σ(C3-C4)	74.9 (n)
	II	0.615 *n*(N2) - 0.502 *n*(O1) - 0.274 *n*(O6) - 0.269 π(C3-O6)	75.8 (n)
	III	0.486 *n*(N7) + 0.418 *n*(N2) - 0.410 *n*(O6) - 0.366 *n*(O1) + 0.299 σ(C3-C4)	72.1 (n)
	IV	0.610 *n*(N2) + 0.454 *n*(O1) - 0.373 *n*(N7) - 0.275 π(C3-O6)	73.9 (n)
	V	0.521 *n*(N7) + 0.447 *n*(N2) - 0.392 *n*(O6) + 0.308 σ(C3-C4) – 0.250 π(C3-O6)	70.2 (n)
	VI	0.636 *n*(N7) - 0.483 *n*(O6) + 0.353 σ(C3-C4) + 0.288 *n*(N2)	74.5 (n)
	VII	0.616 *n*(N2) - 0.504 *n*(O1) - 0.311 *n*(O6) - 0.282 π(C3-O6)	75.5 (n)
HOMO-1 (19*a*)	I	0.504 *n*(N2) - 0.489 *n*(N7) - 0.354 *n*(O1) - 0.336 π(C3-O6)	69.6 (n)
	II	0.837 *n*(N7) + 0.320 σ(C4-H12)	74.8 (n)
	III	0.535 *n*(N2) - 0.503 *n*(N7) - 0.362 *n*(O1) - 0.257 π(C3-O6) + 0.255 *n*(O6)	76.6 (n)
	IV	0.741 *n*(N7) + 0.284 *n*(N2) - 0.238 *n*(O6) - 0.227 σ(C5-C4)	73.0 (n)
	V	0.511 *n*(N2) + 0.456 *n*(O1) - 0.418 *n*(N7) + 0.261 *n*(O6)- 0.251 π(C3-O6)	72.0 (n)
	VI	0.616 *n*(N2) + 0.491 *n*(O1) - 0.363 π(C3-O6)	69.9 (n)
	VII	0.853 *n*(N7) + 0.335 σ(C4-H12)	77.4 (n)
HOMO-2 (18*a*)	I	0.676 *n*(O6) + 0.595 *n*(N7)	84.7 (n)
	II	0.717 *n*(O6) - 0.347 σ(C3-C4) + 0.236 *n*(N2)	62.4 (n)
	III	0.627 *n*(O6) + 0.577 *n*(N7) - 0.262 π(C3-O6)	75.9 (n)
	IV	0.731 *n*(O6) - 0.352 σ(C3-C4) + 0.262 *n*(N7)	66.2 (n)
	V	0.672 *n*(O6) + 0.605 *n*(N7)	83.6 (n)
	VI	0.629 *n*(O6) + 0.607 *n*(N7)	80.5 (n)
	VII	0.698 *n*(O6) - 0.326 σ(C3-C4) + 0.236 *n*(N2)	63.4 (n)
HOMO-3 (17*a*)	I	0.500 π(C3-O6) - 0.429 *n*(O1) + 0.398σ(C5-H9) + 0.395 σ(C4-H12) - 0.329 σ(C5-C4)	75.2 (b)
	II	0.537 π(C3-O6) - 0.482 *n*(O1) + 0.429σ(C5-H9) - 0.294 *n*(N7) - 0.248 σ(C5-C4)	63.4 (b)
	III	0.505 π(C3-O6) - 0.468 *n*(O1) + 0.433σ(C5-H10) - 0.278 σ(C5-C4) + 0.250 σ(C4-N7) + 0.228 *n*(O6)	67.4 (b)
	IV	0.519 π(C3-O6) + 0.509 *n*(O1) - 0.424σ(C5-H9) + 0.246 *n*(N7) + 0.234σ(C5-H10) + 0.227 σ(C5-C4)	61.7 (b)
	V	0.520 π(C3-O6) + 0.428 *n*(O1) - 0.388 σ(C5-H9) - 0.366 σ(C4-H12) + 0.314 σ(C5-C4)	72.9 (b)
	VI	0.548 π(C3-O6) + 0.490 *n*(O1) - 0.412 σ(C5-H10) - 0.246 σ(C4-N6) + 0.245 σ(C5-C4)	68.4 (b)
	VII	0.554 π(C3-O6) - 0.482 *n*(O1) + 0.422σ(C5-H10) + 0.261 σ(C4-N6) - 0.251 σ(C5-C4)	69.9 (b)
HOMO-4 (16*a*)	I	0.433 σ(C5-C4) + 0.402 *n*(O1) - 0.346 σ(C4-N7) - 0.334 σ(C5-H10) + 0.327 σ(N7-H13) + 0.320 π(C3-O6) - 0.257 *n*(O6) - 0.229 σ(C5-O1)	74.9 (b)
	II	0.409 *n*(O1) - 0.402 σ(C4-N7) + 0.399 σ(C5-C4) - 0.324 σ(C5-H10) + 0.280 σ(N7-H13) - 0.256 *n*(O6) + 0.247 π(C3-O6) - 0.238 σ(C5-O1)	70.9 (b)
	III	0.541 σ(C4-H12) - 0.408 σ(C5-C4) - 0.346 *n*(O1) - 0.310 π(C3-O6) + 0.260 σ(N7-H8) + 0.231 σ(C5-O3)	81.0 (b)
	IV	0.455 *n*(O1) + 0.398 σ(C5-C4) - 0.381 σ(C4-N7) - 0.353 σ(C5-H10) - 0.286 *n*(O6) + 0.272 σ(N7-H13) - 0.254 σ(C5-O3)	66.1 (b)
	V	0.430 *n*(O1) - 0.421 σ(C5-H10) + 0.412 σ(C5-C4) + 0.319 σ(N7-H13) - 0.256 σ(N2-O1)	68.4 (b)
	VI	0.525 σ(C4-H12) - 0.413 *n*(O1) - 0.402 σ(C5-C4) + 0.301 σ(C5-O1) + 0.252 σ(N7-H8) + 0.247 *n*(O6) - 0.230 σ(N7-H13)	73.0 (b)
	VII	0.444 σ(C5-C4) + 0.407 *n*(O1) + 0.392 π(C3-O6) - 0.304 σ(C4-H12) + 0.294 *n*(N7) - 0.244 σ(C5-H9) - 0.229 σ(C5-O3)	66.1 (b)

[1] NBO coefficients whose values of c^2 are ≥ 0.05 (5% contribution to the MO).
[2] Percentage contribution of the dominant character of the MO (b = bonding, n = nonbonding).

Table 2 Vertical IE (eV) and Pole Strength (in parenthesis) of the seven most stable conformers (I-VII) of D-cycloserine calculated by the OVGF/6-311++G** method.

MO	IE (I)	IE (II)	IE (III)	IE (IV)	IE (V)	IE (VI)	IE (VII)
20*a* (HOMO)	9.24 (0.904)	9.38 (0.900)	9.20 (0.903)	9.57 (0.902)	9.54 (0.904)	9.45 (0.906)	9.29 (0.899)
19*a*	9.96 (0.901)	10.09 (0.910)	10.02 (0.901)	10.07 (0.908)	9.72 (0.902)	9.66 (0.898)	10.12 (0.911)
18*a*	11.30 (0.899)	10.63 (0.900)	11.26 (0.898)	10.59 (0.902)	11.19 (0.899)	11.34 (0.899)	10.62 (0.900)
17*a*	12.13 (0.903)	12.28 (0.899)	12.40 (0.899)	12.29 (0.900)	12.25 (0.903)	12.41 (0.899)	12.32 (0.898)
16*a*	13.57 (0.901)	13.60 (0.902)	13.19 (0.906)	13.63 (0.903)	13.51 (0.905)	13.29 (0.907)	13.58 (0.899)
15*a*	14.40 (0.901)	14.24 (0.895)	14.46 (0.894)	13.96 (0.891)	13.81 (0.893)	13.97 (0.896)	14.20 (0.899)
14*a*	14.43 (0.896)	14.51 (0.898)	14.60 (0.903)	14.22 (0.904)	14.54 (0.902)	14.87 (0.900)	14.55 (0.899)
13*a*	14.78 (0.901)	15.08 (0.906)	15.12 (0.903)	15.03 (0.898)	14.91 (0.897)	14.94 (0.901)	15.08 (0.902)
12*a*	15.52 (0.900)	15.23 (0.893)	15.32 (0.899)	15.74 (0.901)	16.09 (0.906)	15.35 (0.895)	15.01 (0.897)
11*a*	16.23 (0.893)	15.92 (0.899)	15.81 (0.897)	16.16 (0.895)	16.11 (0.893)	16.21 (0.895)	15.84 (0.898)
10*a*	16.78 (0.902)	16.60 (0.900)	16.59 (0.893)	16.62 (0.903)	16.59 (0.900)	16.66 (0.899)	17.04 (0.901)
9*a*	16.92 (0.886)	17.55 (0.893)	17.66 (0.891)	17.55 (0.891)	17.36 (0.886)	17.53 (0.893)	17.43 (0.893)
8*a*	18.28 (0.890)	18.13 (0.888)	17.94 (0.891)	18.19 (0.890)	18.24 (0.893)	17.92 (0.890)	17.85 (0.890)

Cite this: DOI: 10.1039/c0xx00000x

www.rsc.org/xxxxxx

ARTICLE TYPE

3. Results and discussion

3.1 - Valence electronic structure

The valence electronic structure of D-cycloserine, and its dependence on conformational flexibility were investigated by calculating the valence IEs and the associated pole strengths. To this end, we used the OVGF method,[16-20] and included the seven most stable conformers I-VII of D-cycloserine located at the MP2/6-311++G** level of theory. The theoretical data allowed to simulate the UPS in terms of partial contributions of the various conformers. The theoretical simulation was combined with the detailed analysis of the occupied MOs (see Table 1), and compared with the experimental UPS.[11] This provided a comprehensive band assignment, and shed light into the contribution of each conformer to the observed spectral features.

3.1.1 Calculated outer valence photoelectron spectrum

The OVGF IEs in the outer valence region (IE < 20 eV), and the corresponding pole strengths for the ionizations involving the thirteen outermost MOs of the I-VII conformers of D-cycloserine, from 8*a* to 20*a* (HOMO), are listed in Table 2. We first note that the pole strengths are invariably quite large and within 0.90 ± 0.01. This confirms the validity of the one-particle picture in describing the ionization processes of the closed-shell D-cycloserine within the OVGF method, and the consequent expected accuracy of the theoretical vertical IEs. The valence UPS of any single conformer was simulated by convolving its spectral lines (defined by the vertical IE and pole strength) with Gaussian functions whose FWHM was arbitrarily set at 0.5 eV. The simulated UPS of D-cycloserine is then obtained by summing the spectra of the various conformers weighted by the calculated Boltzmann factors at the experimental temperature (see Fig. 1). The outer valence spectrum of D-cycloserine simulated in this way is shown in Figs. 2 and 3 (black solid line) together with the contributions of the conformers I-VII. In the 9-11.5 eV IE range, the outermost valence region exhibits three main components, labelled as A-C in Fig. 3. They arise from the ionization of the HOMO (20*a*), HOMO-1 (19*a*) and HOMO-2 (18*a*) of the various conformers. The partial contribution of each group of ionizations is reported in the figure according to the specific MO involved. Interestingly, the calculated spectrum points out that the effect of the conformational flexibility on the ionization of D-cycloserine sensibly depends on the nature of the involved MO. Thus, for processes associated with the 18*a* MO, the IEs of conformers I-VII are spread over an energy range which is much larger than that of the ionizations involving the HOMO and HOMO-1. This is also evident by comparing the vertical IEs (see Table 2) of the 20a, 19a and 18a MOs, whose energy ranges are 0.37, 0.46, and 0.75 eV, respectively. For processes involving the HOMO-3 (17*a*) and associated with the spectral feature D, the vertical IE is instead nearly insensitive to the conformational change, the IEs of conformers I-VII for this MO (see Table 2) falling within 0.28 eV, which is the smallest IE range in the outer valence spectrum.

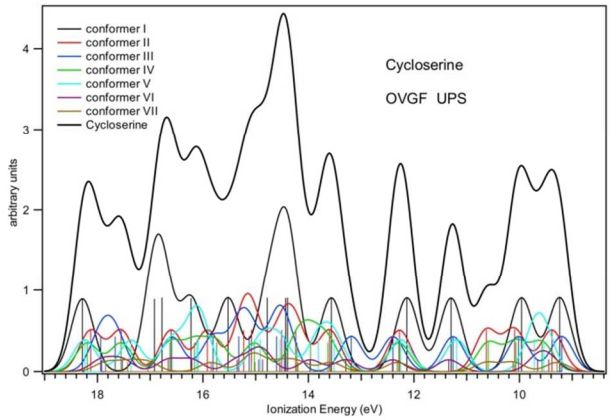

Fig. 2 The outer valence UPS of D-cycloserine at T = 395K calculated by the OVGF method (thick black curve). The spectral components of the most stable conformers I-VII are reported as curves of different colors. The vertical bars correspond to the calculated IEs and relative intensities. The spectral lines are convoluted using Gaussian functions of 0.5 eV FWHM (see text).

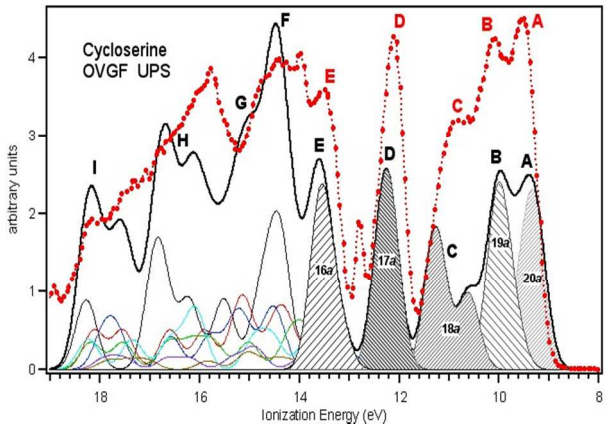

Fig. 3 The outer valence UPS of D-cycloserine calculated at T = 395K (black curve). The contribution of the ionization of conformers I-VII is reported as a function of the involved MO. The assignment of the five outermost bands (A-E) is also reported. Labels A-I refer to the spectral features observed in the experiment of Ref. 11. The experimental UPS (red dots) is also reported on the same IE scale, shifted by +0.2 eV, for comparison (weak feature at 12.6 eV is due to H_2O impurities). Adapted with permission from Ref. 11. Copyright (2014) American Chemical Society.

As far as the spectral assignment is concerned, although 20*a* and 19*a*, and 19*a* and 18*a* components partially overlap, three clear peak maxima, A, B and C, are discerned at 9.39, 9.96, and 11.27 eV, respectively. A forth well separated band, labelled D, is observed at higher energies with vertical IE of 12.25 eV, which is assigned to the ionization of the 17*a* MO of conformers I-VII. The next spectral feature, E, is observed at higher energies as a

band peaked at 13.61 eV IE, and mainly assigned to ionization of the 16*a* MO of the conformers. It should be noticed that the overlap between different spectral components becomes stronger and stronger on going from feature E to I (see Fig. 2) due to the higher density of states predicted at larger IE values. This makes difficult, in this spectral region, a clear band assignments in terms of ionizations of specific MOs.

3.1.2 - MO analysis

The HF/6-311++G** canonical MOs of the conformers I-VII of D-cycloserine are reported in Table 2 in terms of their leading NBO contributions. The included MOs from 20*a* to 16*a* are those associated with the five outermost valence ionization processes, and account for the most relevant part of the UPS.

The HOMO of any conformer is delocalized on the nitrogen (N_2 and N_7) and the oxygen (O_1 and O_6) atoms, and is essentially non-bonding (ca. 75%, see Table 2). Significant but relatively smaller contributions come from the $\pi_{C=O}$ (particularly in II, IV, V, and VII) and the σ_{C3-C4} (particularly in I, III, V, and VI). The HOMO-1 of I-VII is also delocalized and predominantly non-bonding. Leading contributions come from N_2 and N_7, and O_1 and O_6, the former being significantly larger. We note also a substantial contribution of the $\pi_{C=O}$ in conformers I, III, IV, and V, and smaller contributions of σ_{C4-H12} and σ_{C4-C5}, respectively, in conformers II and VI, and IV. The HOMO-2 is as well invariably predominantly non-bonding, and features a largest contribution of n_{O6} (I-VII) or comparably large contributions of n_{O6} and n_{N7} (I, III, V, and VI). We also note the smaller contributions of σ_{C3-C4} in II, IV, and VII. There is, however, no appreciable contribution from the endocyclic oxygen atom (O_1). The outermost occupied MO with predominantly bonding character is the HOMO-3, which invariably features the largest contribution of the $\pi_{C=O}$, and additional contributions from the σ_{C-H} of the CH_2 group, and the σ_{C5-C4}. The minor non-bonding character of this MO essentially reflects the relatively large contribution of n_{O1}. The HOMO-4 is mainly bonding, and features the largest degree of delocalization among the five outermost occupied MOs. Contributing orbitals include the σ_{C-C}, σ_{C-N}, σ_{C-O}, σ_{N-H}, σ_{C-H}, and, especially for the most stable I, II and III, the $\pi_{C=O}$. The minor non-bonding contribution comes from the n_{O1}.

The frontier MOs of a group of biologically-active compounds, including D-cycloserine, were recently investigated at B3LYP/6-311G** DFT level of theory,[10] and the LUMO was identified as an effective indicator of agonist or antagonist activity toward the $Glycine_B$-iGluR-NMDA receptor. In particular, like other identified agonists, for the D-cycloserine this orbital was described as largely localized on the carbonyl group. Thus, we felt of interest to further probe here this assignment, paying particular attention to the conceivable effect of the basis set. As a matter of fact, at the HF/6-311G** level of theory (*i.e.* without diffuse functions), the LUMO of the most stable conformer of D-cycloserine (I) resulted to have a non-bonding/anti-bonding mixed character, the former arising from the contribution of the ring H atoms H_8, H_{10}, and H_{12}, and the latter arising from the C=O and C_4-H_{12} bonds. This description is strictly similar to that obtained at the B3LYP/6-311G** level of theory (see Fig. 3f of Ref. 10). However, when diffuse functions on the heteroatoms are included (HF/6-311+G**), the LUMO becomes predominantly non-bonding (91%) with main contributions from C_3 and C_4. Finally, when diffuse functions are also included to the hydrogen atoms (HF/6-311++G**), the non-bonding character of the LUMO becomes even larger (93%), and the orbital is mainly composed by functions on the H atoms, with no significant contributions from the heteroatoms. It is worth mentioning that the use of different basis sets leaves essentially unaffected the composition of the occupied MOs (they feature, in fact, negligible contributions from the atomic polarization functions).

3.1.3 - Experimental outer valence UPS assignment

The theoretical results provide a rational basis to assign the experimental outer valence photoelectron spectrum of D-cycloserine. In particular, if one refers to the spectrum recorded in the vapor phase at 395 K (Fig. 6 of Ref. 11), in the low IE region it includes three strong bands detected as two maxima (A and B) and a shoulder (C), at 9.22, 9.88, and 10.82 eV, respectively. The corresponding region in the simulated spectrum displays three contributions due to the ionizations of the HOMO, HOMO-1 and HOMO-2 of conformers I-VII. The first two components, labeled 20*a* and 19*a* and peaked at 9.34 and 10.00 eV in Fig. 3, are in excellent agreement with the first two experimental bands A and B, and show the same energy separation of 0.66 eV. These two bands are therefore assigned to ionizations from the highly delocalized 20*a* and 19*a* MOs of non-bonding character, as described in the previous section.

The shoulder C observed in the experimental UPS at 10.82 eV IE corresponds to the calculated component C, which exhibits a main peak at 11.26 eV accompanied by a weaker structure centered at 10.63 eV. The experimental shoulder is therefore assigned to ionizations from the non-bonding 18*a* MO. As seen in Table 1, this MO is much less delocalized than the other MOs, being made of fewer contributions which involve only the O_6-C_3-C_4-N_7 molecular fragment. The main non-bonding character (n_{O6} and n_{N7}) is actually mixed with a minor σ_{C3-C4} contribution. For feature C the agreement between the experiment and the simulation is reasonably good, but not as good as for the previous bands. This is not surprising since neither photoionization cross sections nor vibronic structure were taken into account in the spectral simulation. The relative intensities and band shapes of the experimental spectral components might be significantly different from those predicted in the simulated spectrum, where the pole strengths are found nearly constant for all the ionization processes, and the peak shape of all spectral lines was assumed to be a single Gaussian function. It is striking that IEs of different conformers for the spectral component C are predicted to be spread over a much larger energy range than the other ionizations (see Fig. 3). The experimental band of D-cycloserine associated with the 18*a* MO is therefore expected to be substantially affected by excitation of vibrational modes accompanying the photoionization process.

The most intense single feature in the experimental spectrum is displayed at 11.94 eV IE as peak D, which is the only band almost entirely resolved in the spectrum. The simulated spectrum is in excellent agreement with this finding displaying a

single well resolved component at 12.25 eV IE (D). This experimental band is therefore ascribed to ionizations from the highly delocalized 17*a* MO, which at variance with previous MOs, has a main bonding character. This is due to the largest $\pi_{C=O}$ contribution and important σ_{C-H} contributions from the CH_2 moiety. The bonding character is also mixed with a relatively large non-bonding contribution from the endocyclic oxygen (n_{O1}). The next structure displayed in the experimental spectrum is the strong and partially resolved band E, whose maximum is found at 13.28 eV IE. This experimental feature is clearly visible in the calculated spectrum of Fig. 3 as the partially resolved component E, which is assigned to ionizations from the 16*a* MO. This component is peaked at 13.55 eV, and associated with a highly delocalized MO of predominant bonding character (see Table 1) due to σ chemical bonds contributions involving the molecular skeleton H_2N-C-CH_2-O and the $\pi_{C=O}$ contribution. A minor but significant non-bonding contribution to this orbital is also given by n_{O1}. The high IE region of the experimental UPS, namely from 13.5 to 18.0 eV, exhibits the structures labeled F-I. This region corresponds to the spectral simulation calculated from 14.0 to 18.5 eV IE in Fig. 3. As mentioned above, the OVGF theoretical predictions point out a strong overlap between conformer ionizations associated to the eight MOs 15*a* – 8*a*. Although the assignment in terms of single MO cannot be reliably provided in this region, a qualitative agreement between the experimental and calculated spectral intensity pattern is actually observed if one considers structures F-I in Fig. 3 and Fig. 6 of Ref. 11.

3.2 - Core electronic structure

3.2.1 Calculated Core IEs

The vertical IEs of C1s, N1s and O1s core electrons of conformers I-VII were calculated to investigate the effect of the molecular conformational flexibility of D-cycloserine on its gas phase XPS spectra. The IEs obtained using the ΔSCF approach are reported in Table 3, along with the corresponding DFT values obtained by the LB94 potential. The more accurate ΔSCF values have been used to simulate the XPS spectra following the same procedure adopted for the UPS simulation at T = 395 K. The only difference is that spectral lines are convoluted using the same photoionization cross section, reasonably assumed to be equal for core electrons of non-equivalent atoms of the same element. The relative intensities of spectral lines are thus only determined by the Boltzmann factors of the different conformers (see Fig. 1). The simulated XPS spectra, as obtained with Gaussian convolution functions of FWHM arbitrarily set at 0.5 eV, are reported in Figs. 4a-c for the C1*s*, N1*s*, and O1*s* regions, respectively. The calculated vertical IE for the different atomic sites is reported in Table 3 as peak maximum of the convolution curve associated with the conformers contributions. The different chemical shift spread of the I-VII conformers for the atomic components can be clearly observed in the Figs 4a-c by considering the set of IEs of each spectral band. It is worth noting that the predicted chemical shift spread of the atomic XPS components is not sufficiently large to mix the set of core IE values of different atoms, even for the partially overlapping bands of C_4 and C_5 (Fig. 4a).

3.2.2 Experimental XPS assignment

The vertical IEs obtained in the XPS simulations of Figs. 4a-c are in excellent agreement with the experiment, and in qualitative agreement with the assignment derived from a previous simulation.[11] In the case of the C1*s* XPS, the IEs obtained in the simulation for the C_3, C_5 and C_4 atoms are 293.76, 292.70 and 292.20 eV, respectively. These values are found in substantially better agreement with the experiment, in both the absolute values and energy pattern, than in a previously theoretical investigation, where only one conformer of D-cycloserine (particularly III) was taken into account.[11]

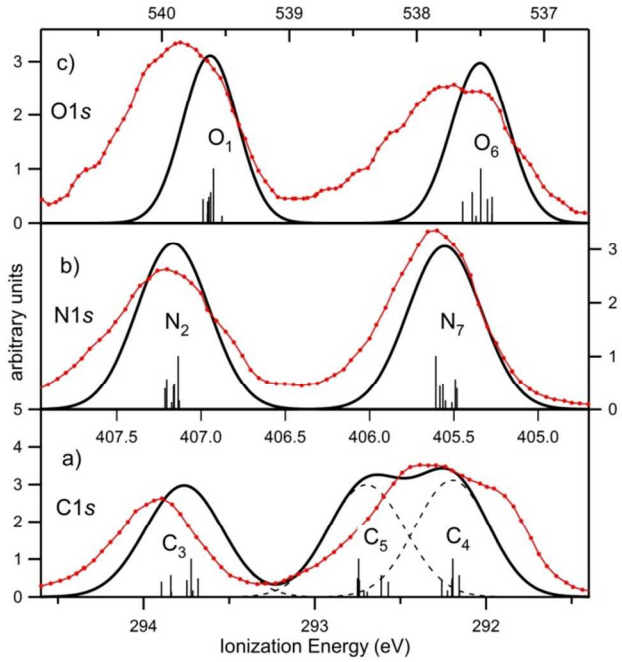

Fig.4 - The XPS calculated for the C1*s* (a), N1*s* (b), and O1*s* (c) ionizations of D-cycloserine (black curves). The IE value spread of the conformers I-VII is reported for each core-ionized atom as vertical bars. The relative intensities of spectral lines (bars' heights) are Boltzmann population factors calculated at T = 395K. The experimental XPS (red dots) are also reported on the same IE scale for comparison. Adapted with permission from Ref. 11. Copyright (2014) American Chemical Society.

Moreover, the C_4 peak in Fig. 4a is slightly more intense than that of C_5 due to its relatively narrower chemical shift spread. Interestingly, a similar partially overlapped structure is also observed in the experiment, but with reverse order of the relative intensities of the two components. Since the C1*s* core hole broadening for the three different C atoms is expected to be approximately constant and of the order of 100 meV,[29,30] the different intensity trends, the one observed in the experiment and that predicted by the simulation, have to be ascribed to a remarkably different vibronic structures of the C_4 and C_5 XPS bands. The observed shape of the two-component peak in the experiment can, in fact, be explained in terms of a vibrationally much broader C_4 component ~~(C_4 in Ref. 11)~~ that appears as intense shoulder at the low IE flank of the unresolved composite feature (see red curve in Fig. 4a).

Table 3 Calculated core electron IE (eV) of conformers I-VII of D-cycloserine.

atomic site	I	II	III	IV	V	VI	VII	IE_{theor} [2]	IE_{exp} [3]
C_4	292.19 (291.51)	292.16 (291.47)	292.20 (291.50)	292.20 (291.50)	292.26 (291.54)	292.23 (291.52)	292.16 (291.46)	292.20	291.9
C_5	292.74 (291.81)	292.61 (291.70)	292.75 (291.80)	292.57 (291.74)	292.74 (291.88)	292.71 (291.85)	292.69 (291.75)	292.70	292.3
C_3	293.72 (292.92)	293.84 (293.02)	293.68 (292.94)	293.90 (293.07)	293.75 (292.94)	293.71 (292.95)	293.84 (292.99)	293.76	293.9
N_7	405.61 (403.40)	405.49 (403.24)	405.57 (403.42)	405.48 (403.22)	405.58 (403.40)	405.55 (403.40)	405.51 (403.27)	405.56	405.6
N_2	407.14 (405.78)	407.20 (405.81)	407.16 (405.78)	407.21 (405.77)	407.16 (405.75)	407.13 (405.73)	407.17 (405.75)	407.17	407.2
O_6	537.50 (534.81)	537.57 (534.87)	537.41 (534.79)	537.64 (534.94)	537.45 (534.82)	537.41 (534.78)	537.54 (534.82)	537.50	537.75
O_1	539.60 (536.71)	539.62 (536.71)	539.63 (536.73)	539.64 (536.71)	539.68 (536.74)	539.64 (536.73)	539.53 (536.59)	539.62	539.85

[1] vertical IE values obtained by the ΔSCF method. Values in parenthesis are obtained using the LB94 potential;

[2] maximum of the simulated spectral component;

[3] experimental vertical IE from Ref. 11.

Cite this: DOI: 10.1039/c0xx00000x

www.rsc.org/xxxxxx

ARTICLE TYPE

The specific vibrational broadening of the individual conformers in the C_4 and C_5 bands plays thus an important role that cannot be neglected to accurately simulate the two experimental XPS components.

Fig. 4b shows the N1*s* ionization peaks associated with the endo- and exo-cyclic nitrogen atoms N_2 and N_7. The derived vertical IEs, 407.17 and 405.56 eV, are coincident with the experimental values of 407.2 and 405.6 eV, respectively (red curve). The two bands are fully resolved in both the simulated and experimental spectra because of the large difference in the IE values (1.61eV). This reflects the large increase in the N1*s* IE arising from the strong mesomeric (-R) and inductive (-I) electron withdrawing effects exerted by the carbonyl group and the oxygen atom (O_1) directly bound to N_2. N_7 core ionizations of conformers I-VII display a larger IE spread. So, this band in Fig. 3b has a slightly lower maximum value than the N_2 peak. At variance with the simulation, the experiment shows two bands of approximately equal area with markedly different peak widths and maximum values where the high IE band exhibits a larger width and lower maximum. This, as mentioned for the C1*s* XPS, is explained by the important effect of the vibrational structure in determining the XPS band shape.

Finally, Fig. 4c shows the simulated O1*s* XPS of D-cycloserine at T = 395K. The calculated core IEs for O_1 and O_6, 539.62 and 537.50 eV, respectively, are in excellent agreement with the experimental ones of 539.85 and 537.75 eV. The core IEs involving the oxygen of the carbonyl group (O_6) and calculated for the I-VII conformers are spread over a much larger energy range than the corresponding values of O_1. This makes the O_6 XPS band larger than that associated with O_1, and with a smaller maximum intensity value (black curve in Fig. 4c). These findings are also observed in the experimental spectrum, where the difference in the peak width and maximum value between the two atomic components is much more pronounced than in the simulated spectrum. In the case of the O1*s* XPS, at variance with the C1*s* and N1*s* cases, both the conformational effect and the vibrational structure contribute with synergistic effects to the band shape difference between the two XPS components.

4. Conclusions

The small but highly flexible D-cycloserine was found to possess twelve stable conformers, I-XII, which are structurally related by the two isoxazolidine ring puckering conformations, the axial/equatorial positions of the N_2-H_{11} bond in the ring, and the rotation of the NH_2 moiety around the C_4-N_7 bond. The subset of the seven most stable conformers I-VII was assumed to properly describe the properties of the D-cycloserine. In fact, based on calculated Boltzmann populations, the ensemble of gas phase molecules in thermal equilibrium at 395 K is nearly totally composed (97%) by these conformers. The simple inclusion of conformers III and VII adopted in previous studies[11], which was caused by an incorrect description of the five-member ring flexibility, is expected to provide a rather poor description of the molecular properties, as these isomers account for only 18% of the probed sample (as a matter of fact, the most stable I and II account for 48% of the population). Therefore, the present investigation was aimed at providing the first comprehensive description of the role played by the conformational flexibility in the valence and core electronic structures of the D-cycloserine by simulating the corresponding UPS and XPS spectra, where the full set of structural degrees of freedom is taken into account.

In the case of the UPS, the comparison between the simulated and experimental spectra provided a substantially better quantitative agreement between the calculated IE pattern and the experiment than that reported in a recent study.[11] The outermost spectral region, denoted as structures A-E in Fig. 3, was assigned to the ionization of the five highest occupied MOs 20*a*-16*a* of conformers I-VII, and the analysis of the relevant MOs was provided in terms of leading NBO contributions. At variance with previous investigations, the HOMO[10,11] resulted invariably predominantly non-bonding (~75%), and largely delocalized on the four nitrogen and oxygen atoms. Relatively smaller contributions come also from the NBOs $\pi_{C=O}$ (conformers II, IV, V, and VII), and σ_{C3-C4} (conformers I, III, V, and VI). The HOMO-1 and HOMO-2 of conformers I-VII are also mainly non-bonding, and the HOMO-3 is mainly bonding (NBOs $\pi_{C=O}$). The HOMO-4 has also a mainly bonding character, but with contributions from σ NBOs larger than those from $\pi_{C=O}$ NBOs.

As for the XPS spectra, the C1*s*, N1*s*, and O1*s* calculated IEs for the conformers I-VII has allowed to evaluate, in the spectral simulations, the IE chemical shift spread associated to the conformational flexibility of D-cycloserine for each XPS band. This IE spread turned out to be not sufficiently large to cause mixing of XPS components. The vertical IE values derived from the simulated spectra were generally in substantially better agreement with the experimental XPS as for both the absolute values and energy patterns. The spectral simulations point out different band broadenings of the various XPS components due to the different sensitivity to the conformational flexibility of their IE chemical shifts. While agreement is found between the simulated and experimental O1*s* XPS spectra, predictions of the simulated N1*s* and C1*s* XPS show a reverse trend of the relative peak broadenings and maxima with respect to the experiment. This is ascribed to the different vibrational widening of the conformer components in the different XPS bands, since this effect is not included in the simulation method.

Acknowledgements

Work supported by the Ministero dell'Istruzione dell'Università e della Ricerca of Italy (PRIN 2010-2011: CUP B81J1200283001). Annito Di Marzio is gratefully acknowledged for technical assistance.

5. Notes and references

[a]*Dipartimento di Chimica e Tecnologie del Farmaco, Università "Sapienza", P.le A. Moro 5, 00185, Roma, Italy. Fax: 0039-06-49913602 e-mail: antonello.filippi@uniroma1.it*
[b]*Dipartimento per la Innovazione nei sistemi Biologici, Agroalimentari e Forestali (DIBAF), Università della Tuscia, L.go dell'Università, s.n.c., 01100, Viterbo, Italy*
[c]*Dipartimento di Scienze Chimiche e Farmaceutiche, Università degli studi di Trieste, Via L. Giorgieri 1, I-34117 Trieste, Italy*
[d]*IOM-CNR, Tasc Laboratory, Area Science Park, Basovizza, Trieste, Italy. e-mail: stefano.stranges@uniroma1.it*

† Electronic Supplementary Information (ESI) available: Cycloserine Conformers: Geometry Descriptors and Cartesian Coordinates. See DOI: 10.1039/b000000x/

1 F. D. Lowy, *J. Clin. Invest.,* 2003, **111**, 1265.
2 R. Dall'Olio, O. Gandolfi, R. Gaggi, *Behav. Pharmacology,* 2000, **11**, 631.
3 G. Kaushal, R. Ramirez, D. Alambo, W. Taupradist, K. Choksi, C. Sirbu, *Drug Discoveries & Therapeutics,* 2011, **5**, 253.
4 S. G. Hoffmann, A. E. Meuret, J. A. Smith, N. M. Simon, M. H. Pollack, K. Eisenmenger, M. Shiekh, M. W. Otto, *Arch. Gen. Psychiatry,* 2006, **63**, 298.
5 M. W. Otto, D. F. Olin, N. M. Simon, G. D. Pearlson, S. Basden, S. A. E. Meunier, S. G. Hoffmann, K. Eisenmenger, J. H. Krystal, M. H. Pollack, *Biol. Psychiatry,* 2010, **67**, 365.
6 G. S. Chasson, U. Buhlmann, D. F. Tolin, S. R. Rao, H. E. Reese, T. Rowley, K. S. Welsh, S. Wilhelm, *Behav. Res. Ther.,* 2010, **48**, 675.
7 M. G. Kushner, S. W. Kim, C. Donahue, P. Thuras, D. Adson, M. Kotlyar, J. McCabe, J. Peterson, E. B. Foa, *Biol. Psychiatry,* 2007, ***62***, 835.
8 F. Kuehl, Jr., F. J. Wolf, N. R. Trenner, R. L. Peck, R. P. Buhs, I. Putter, R. Ormond, J. E. Lyons, L. Chaiet, E. Howe, et al., *J. Amer. Chem. Soc.,* 1955, **77**, 2344.
9 L. F. Iakhontova, B. P. Bruns, V. D. Kartseva, S. N. Kobzieva, N. A. Perevozskaia, *Antibiotiki,* 1969, **14**, 205.
10 J. Yosa, M. Blanco, O. Acevedo, L. R. Lareo, *Eur. J. Med. Chem.* 2009, **44**, 2960.
11 M. Ahmed, F. Wang, R. G. Acres, K. C. Prince, *arXiv.org, e-Print Archive, Physics,* 2013, 1-28, arXiv:1305.6384v1 [physics.chem-ph]; M. Ahmed, F. Wang, R. G. Acres, K. C. Prince, *J. Phys, Chem. A,* 2014, **118**, 3645.
12 C. Fraschetti, A. Filippi, S. Borocci, V. Steinmetz, M. Speranza, *ChemPlusChem,* 2014**, 79**, 584.
13 J. S. Binkley, J. A. Pople, *Int. J. Quantum Chem.,* 1975, **9**, 229.
14 M. W. Schmidt, K. K. Baldridge, J. A. Boatz, S. T. Elbert, M. S. Gordon, J. H. Jensen, S. Koseki, N. Matsunaga, K. A. Nguyen, S. J. Su, T. L. Windus, M. Dupuis, J. A. Montgomery, *J. Comput. Chem.,*1993, **14**, 1347.
15 M. S. Gordon, M. W. Schmidt, *Advances in electronic structure theory: GAMESS a decade later*, 2005, p. 1167, in *Theory and Applications of Computational Chemistry: the first forty years,* C. E. Dykstra, G. Frenking, K. S. Kim, G. E. Scuseria (editors), Elsevier, Amsterdam.
16 L. C. Cederbaum, *J. Phys. B: At. Mol. Phys.,* 1975, **8**, 290.
17 W. Von Niessen, J. Schirmer, L. C. Cederbaum, *Comput. Phys. Rep.,* 1984, **1**, 57.
18 V. G. Zakrzewski, J. V. Ortiz, J. A. Nichols, D. Heryadi, D. L. Yeager, J. T. Golab, *Int. J. Quantum Chem.,* 1996, **60**, 29.
19 J. Schirmer, L. S. Cederbaum, and O. Walter, *Phys. Rev. A,* 1983, **28**, 1237.
20 D. Danovich, *WIREs Comput. Mol. Sci.*, 2011, **1**, 377.
21 M. J. Frisch, G. W. Trucks, H. B. Schlegel, G. E. Scuseria, M. A. Robb, J. R. Cheeseman, J. A. Jr Montgomery, T. Vreven, K. N. Kudin, J. C. Burant, J. M. Millam, S. S. Iyengar, J. Tomasi, V. Barone, B. Mennucci, M. Cossi, G. Scalmani, N. Rega, G. A. Petersson, H. Nakatsuji, M. Hada, M. Ehara, K. Toyota, R. Fukuda, J. Hasegawa, M. Ishida, T. Nakajima, Y. Honda, O. Kitao, H. Nakai, M. Klene, X. Li, J. E. Knox, H. P. Hratchian, J. B. Cross, C. Adamo, J. Jaramillo, R. Gomperts, R. E. Stratmann, O. Yazyev, A. J. Austin, R. Cammi, C. Pomelli, J. W. Ochterski, P. Y. Ayala, K. Morokuma, G. A. Voth, P. Salvador, J. J. Dannenberg, V. G. Zakrzewski, S. Dapprich, A. D. Daniels, M. C. Strain, O. Farkas, D. K. Malick, A. D. Rabuck, K. Raghavachari, J. B. Foresman, J. V. Ortiz, Q. Cui, A. G. Baboul, S. Clifford, J. Cioslowski, B. B. Stefanov, G. Liu, A. Liashenko, P. Piskorz, I. Komaromi, R. L. Martin, D. J. Fox, T. Keith, M. A. Al-Laham, C. Y. Peng, A. Nanayakkara, M. Challacombe, P. M.W. Gill, B. Johnson,W. Chen, M. W. Wong, C. Gonzalez, J. A. Pople, *Gaussian 03, Revision C.02*., Gaussian, Inc.: Wallingford CT, 2004.
22 F. Weinhold, *J. Comput. Chem.,* 2012, **33**, 2363, and references therein.
23 E. D. Glendening, J. K. Badenhoop, A. E. Reed, J. E. Carpenter, J. A. Bohmann, C. M. Morales, C. R. Landis, F. Weinhold, *NBO 6.0*; Theoretical Chemistry Institute, University of Wisconsin: Madison, 2013.
24 G. te Velde, F. M. Bickelhaupt, E. J. Baerends, C. Fonseca Guerra, S. J. A. van Gisbergen, J. G. Snijders, and T. Ziegler, *J. Comput. Chem.,* 2001, **22**, 931.
25 C. Fonseca Guerra, J. G. Snijders, G. te Velde, and E. J. Baerends, *Theor. Chem. Acc*., 1998, **99**, 391.
26 ADF2010, SCM, Theoretical Chemistry, Vrije University, Amsterdam, The Netherlands.
27 S. Saha, F. Wang, J. B. MacNaughton, A. Moewes, D. P. Chong, *J. Synchrotron Radiat.,* 2008, **15**, 151; A. Thompson, S, Saha, F. Wang, T. Tsuchimochi, A. Nakatata, Y. Imamura, H. Nakai, *Bull. Chem. Soc. Jpn.,* 2009, **82**, 187.
28 Y. Takahata and D. P. Chong, *J. Electron Spectrosc. Relat. Phenom*., 2003, **133**, 69.
29 M. Alagia, M. Lavollee, R. Richter, U. Ekström, V. Carravetta, D. Stranges, B. Brunetti, S. Stranges, *Phys. Rev. A,* 2007, **76**, 022509.
30 C. Nicolas, C. Miron, *J. Electron Spectrosc. Relat. Phenom*., 2012, **185**, 267.